

# Core-shell polycationic polyurea pharomadendrimers: New-generation of sustainable broad-spectrum antibiotics and antifungals

*Sandra N. Pinto*<sup>1§</sup>, *Dalila Mil-Homens*<sup>1§</sup>, *Rita F. Pires*<sup>1</sup>, *Marta M. Alves*<sup>2</sup>,  
*Gabriel Serafim*<sup>1</sup>, *Nuno Martinho*<sup>1</sup>, *Manuel Melo*<sup>3</sup>, *Arsénio M. Fialho*<sup>1,4</sup>  
and *Vasco D.B. Bonifácio*<sup>1,4\*</sup>

<sup>1</sup>iBB-Institute for Bioengineering and Biosciences and i4HB-Institute for Health and Bioeconomy, Instituto Superior Técnico, Av. Rovisco Pais, 1049-001 Lisboa, Portugal.

<sup>2</sup>Centro de Química Estrutural (CQE), Institute of Molecular Sciences, Instituto Superior Técnico (IST), Universidade de Lisboa, Av. Rovisco Pais, 1049-001 Lisboa, Portugal.

<sup>3</sup>Instituto de Tecnologia Química Biológica António Xavier, Universidade NOVA de Lisboa, Av. da República, 2780-157 Oeiras, Portugal. <sup>4</sup>Bioengineering Department, Instituto Superior Técnico, Av. Rovisco Pais, 1049-001 Lisboa, Portugal. §contributed equally to this work. \*e-mail: [vasco.bonifacio@tecnico.ulisboa.pt](mailto:vasco.bonifacio@tecnico.ulisboa.pt)

## Table of Contents

1. Synthesis of Polyurea Pharomadendrimers and Intermediates
2. Microbial Strains and Growth Conditions
3. Measurement of MIC
4. Measurement of MBC
5. Determination of Growth Curves Using Optical Density Readings
6. *In Vitro* Time-kill Curves
7. Mammalian cell culture
8. Mammalian Cell Cytotoxicity Assays
9. *Galleria mellonella* Toxicity Assays
10. Hemolysis Assay
11. Live Cell Imaging Using Confocal Microscopy
12. Scanning Electron Microscopy (SEM) Imaging
13. PURE<sub>G4</sub>OEI<sub>48</sub> Pharomadendrimer Therapeutics of *Galleria mellonella* Larvae
14. Statistical Analysis
15. Supplementary Figure 1

16. Supplementary Table 1
17. Supplementary Figure 2
18. Supplementary Figure 3
19. Supplementary Figure 4
20. Supplementary Figure 5
21. Supplementary Figure 6
22. Supplementary Figure 7
23. Supplementary Video 1
24. Supplementary Video 2

### Synthesis of Polyurea Pharmadendrimers and Intermediates

The synthesis of PURE dendrimers (pharmadendrimers' core), generations 3 to 5, was performed following our previous protocols.<sup>1,2</sup> The synthesis of L-OEI-h (component of the pharmadendrimers shell) also followed our protocol.<sup>3</sup> The synthesis of **PURE<sub>G4</sub>OEI<sub>48</sub>** is briefly described as an example. PURE<sub>G4</sub>OEtOx<sub>48</sub> (1.5 g), previously synthesized,<sup>4</sup> was placed in a 50 mL round bottom flask with 4.8 mL of HCl 5M, and the mixture was heated at 100 °C under stirring for 24 hours. After this period the product precipitated, and the mixture was filtered under vacuum, washed with acetone and a beige solid was isolated. The product was stored at room temperature. The product is hygroscopic and was always dried in vacuum before use.

**PURE<sub>G4</sub>OEI<sub>48</sub>**: Yield: 96%. IR (KBr):  $\nu$  (cm<sup>-1</sup>) 3425 (NH), 2980, 2677, 2433, 2027, 1610 (C=O, urea), 1476, 1060, 814. <sup>1</sup>H NMR (400 MHz, D<sub>2</sub>O)  $\delta$  (ppm): 4.01 (s), 3.87–3.50 (m), 3.44 (s), 3.42–2.86 (m). <sup>13</sup>C NMR (100 MHz, D<sub>2</sub>O)  $\delta$  (ppm): 161.12 (C=O, urea), 56.45, 49.76, 44.58, 43.46 (OEI), 36.38, 35.25; UV-Vis (H<sub>2</sub>O):  $\lambda_{\max}$  = 350 nm. Fluorescence (H<sub>2</sub>O):  $\lambda_{\text{em}}$  = 418.5 nm. *M<sub>w</sub>* (calculated by <sup>1</sup>H NMR): 82871 gmol<sup>-1</sup>.  
**PURE<sub>G3</sub>OEI<sub>24</sub>**: Yield: 95%. <sup>1</sup>H NMR (400 MHz, D<sub>2</sub>O)  $\delta$  (ppm): 4.00 (s), 3.85–3.50 (m), 3.44 (s), 3.45–2.87 (m). *M<sub>w</sub>* (calculated by <sup>1</sup>H NMR): 44439 gmol<sup>-1</sup>. **PURE<sub>G5</sub>OEI<sub>96</sub>**: Yield: 94%. <sup>1</sup>H NMR (400 MHz, D<sub>2</sub>O)  $\delta$  (ppm): 4.01 (s), 3.86–3.51 (m), 3.45 (s), 3.43–2.85 (m). *M<sub>w</sub>* (calculated by <sup>1</sup>H NMR): 160788 gmol<sup>-1</sup>.

### Microbial Strains and Growth Conditions

*Staphylococcus aureus* ATCC 6538 was purchased from the American Type Culture Collection (ATCC, Rockville, MD, USA). *Staphylococcus aureus* JE2 (also referred to as USA300 JE2),<sup>5</sup> *Streptococcus pneumoniae* JNR7/87 (TIGR4),<sup>6</sup> *Pseudomonas*

*aeruginosa* PAO1,<sup>7</sup> *Salmonella enterica* serovar Typhimurium SL1344,<sup>8</sup> *Burkholderia cenocepacia* J2315,<sup>9</sup> *Candida albicans* SC5314<sup>10</sup> and *Candida glabrata* KUE100,<sup>11</sup> are regularly used in our lab. The *Acinetobacter baumannii* C475758 is a clinical strain isolated from a human bronchial aspirate from Hospital de Braga, Braga, Portugal, carbapenem resistant. Bacterial cultures were inoculated in either Luria–Bertani (LB) broth (Conda, Pronadisa) or Mueller-Hinton broth (MHB) (Difco), at 37 °C with aeration, with exception of *Streptococcus pneumoniae* strain that was grown in Todd Hewitt medium, supplemented with 0.5% yeast extract (THY) at 37°C without aeration. *Candida albicans* SC5314 and *Candida glabrata* KEU100<sup>12</sup> were cultivated in rich Yeast Extract-Peptone-Dextrose (YPD) medium or RPMI 1640 medium.

### Measurement of MIC

MICs were determined by the broth microdilution technique according with Clinical and Laboratory Standards Institute (CLSI) guidelines.<sup>13</sup> Briefly, the assay was carried out with an initial bacterial inoculum of  $5 \times 10^5$  and  $1 \times 10^6$  colony forming units (CFU) per mL in RPMI and MHB media, respectively for *Candida* and bacteria cells. Two-fold serial dilution of PURE<sub>G4</sub>OEI<sub>48</sub> (in RPMI or MHB) were then added to a polystyrene 96-well tissue culture plate (Orange) containing the bacterial inoculum. Final *Candida* and bacteria inoculum in each well were diluted to  $2.5 \times 10^5$  and  $5 \times 10^5$  CFU mL<sup>-1</sup>, respectively. The 96-well tissue culture plates were incubated for 18–20 h at 37 °C. MIC is defined as the lowest drug concentration that prevents visible growth of bacteria or fungi.

For MICs determination in the presence of serum, the dendrimer was incubated either in RPMI or MBH containing 10% (v/v) fetal bovine serum (FBS) (Difco) or 10% (v/v) heat inactivated FBS (HI-FBS) (Difco).<sup>14</sup> [REFs [10.1038/s41598-020-80540-6](https://doi.org/10.1038/s41598-020-80540-6)].

### Measurement of MBC

MBCs were determined by a traditional colony count assay.<sup>15</sup> At the end of the MIC assay, 20 µL samples from each well (corresponding to  $\frac{1}{2} \times \text{MIC}$ , MIC,  $2 \times \text{MIC}$ ,  $3 \times \text{MIC}$  of L-OEI-h) were transferred to a new 96-well plate and successively diluted (10-fold). Then, each dilution was sub-cultured in Tryptic Soy Agar (TSA) plates. After incubation at 37 °C for 24 h the resulting colonies were counted. The MBC was defined as the minimum drug concentration that causes quantitative cell death (at least 99.9% killing of

the initial inoculum) and thus the assay allowed the determination of the minimum concentration of an agent necessary to achieve a bactericidal effect.

### **Determination of Growth Curves Using Optical Density Readings**

Briefly, final inoculums of  $2.5 \times 10^5$  and  $5 \times 10^5$  CFU mL<sup>-1</sup> (respectively for *Candida* and bacteria cells) were exposed to a 2-fold dilution series of the **PURE<sub>G4</sub>OEI<sub>48</sub>** in RPMI or MHB in a 96-well plate (final volume 200 μL per well). The optical density (OD) at 595 nm was measured in each well as a function of time using a microplate reader (FilterMax F5 (Molecular Devices, Sunnyvale, CA, USA)). Positive controls for bacteria cell growth were also included (untreated bacteria and candida cells). OD was plotted against pharmadendrimer concentration.

### ***In Vitro* Time-kill Curves**

Time-kill curves of **PURE<sub>G4</sub>OEI<sub>48</sub>** were determined according to literature.<sup>16</sup> Briefly, final inoculums of  $2.5 \times 10^5$  and  $5 \times 10^5$  CFU mL<sup>-1</sup> (respectively for *Candida* and bacteria cells) were exposed to different doses of **PURE<sub>G4</sub>OEI<sub>48</sub>** (0 μM, 1 MIC and 2 MIC) and incubated at 37 °C. Aliquots at specified time points were taken, serially diluted in MHB or RPMI and plated onto TSA plates. TSA plates were incubated for 24 h at 37 °C and bacterial colonies were counted. Viable cells (CFU mL<sup>-1</sup>) are reported here as percentage of the control (bacterial suspension without **PURE<sub>G4</sub>OEI<sub>48</sub>** exposition).

### **Mammalian cell culture**

The immortalized human bronchial epithelial cell line 16HBE14o- was grown according to literature.<sup>17,18</sup> Briefly, cells were maintained in fibronectin/vitrogen coated flasks in minimum essential medium (MEM) with Earle's salt (Gibco, Thermo Fisher Scientific, Rockford, IL, USA) supplemented with 10% fetal bovine serum (Lonza, Basel, Switzerland), 0.292 g L<sup>-1</sup> L-glutamine (Sigma-Aldrich, St. Louis, MO, USA), and penicillin/streptomycin 100 U mL<sup>-1</sup> (Gibco, Thermo Fisher Scientific, Rockford, IL, USA) in a humidified atmosphere at 37 °C with 5% CO<sub>2</sub>. The VK2 (E6/E7) vaginal epithelial cell line CRL-2616 were grown in Keratinocyte-Serum Free medium (Gibco, Thermo Fisher Scientific, Rockford, IL, USA) with 0.1 ng mL<sup>-1</sup> human recombinant EGF, 0.05 mg mL<sup>-1</sup> bovine pituitary extract, and additional calcium chloride 44.1 mg L<sup>-1</sup>. The cells were grown at 37 °C with a 5% CO<sub>2</sub> atmosphere and 95% humidity.

### **Mammalian Cell Cytotoxicity Assays**

The MTT [3-(4,5 dimethylthiazol-2-yl)-2,5 tetrazolium bromide] assays, based on the method previously described,<sup>19</sup> were used to determine the effect of **PURE<sub>G4</sub>OEI<sub>48</sub>** exposition on cell viability. Briefly, human bronchial epithelial 16HBE14o- and vaginal VK2 (E6/E7) cell lines cells were seeded in 96-well plates (Orange Scientific) at a density of  $1 \times 10^4$  cells/well and left to adhere overnight in a CO<sub>2</sub> incubator (5%) at 37 °C. After cell adhesion medium was changed by fresh medium containing different **PURE<sub>G4</sub>OEI<sub>48</sub>** dilutions. After 24 h, the medium was discarded and 20 μL of MTT (5 mgmL<sup>-1</sup>) were added to each well together with 100 μL of fresh cell medium and incubated at 37 °C for 3.5 h. The formazan crystals formed in the wells were dissolved using 150 μL of MTT solvent (4 mM of HCl, 0.1% of Nondet P-40 in isopropanol). The formation of formazan was monitored by measuring the absorbance at 590 nm in a microplate reader (BMG Labtech, Polar Star Optima). The percentage of viable cells was expressed relatively to the values of untreated cells.

### ***Galleria mellonella* Toxicity Assays**

*Galleria mellonella* larvae were reared in our insectarium on a pollen grain and bee wax diet at 25 °C in darkness. Last instar larvae weighing 250±25 mg was used for the survival experiments. *Galleria mellonella* toxicity assays were based on previously described methodologies<sup>20,21</sup> to determine the effect of **PURE<sub>G4</sub>OEI<sub>48</sub>** exposition on *in vivo* model. Briefly, 5 μL of pharomadendrimer (0-60 μM) was administrated into each larva and injected into the larva hindmost left proleg. For each condition we used 10 larvae, a control group was also included in the assay. The larvae survival was assessed daily during a period of 72 h. Each larva was also scored daily to the *G. mellonella* health index, which scores four main parameters: Larvae activity, cocoon formation, melanization and survival, as described.

### **Hemolysis Assay**

The hemolytic activity of **PURE<sub>G4</sub>OEI<sub>48</sub>** was determined following a reported protocol.<sup>22</sup> Briefly, human red blood cells (hRBCs) obtained from healthy volunteers, were re-suspended in PBS (pH 7.4) according with standard methods.<sup>23</sup> A suspension of 1% hematocrit was incubated with different doses of pharomadendrimer at room temperature for 4 h. After centrifugation (1500 g for 5 min) the absorbance of supernatant was measured at 540 nm (Spectrostar Omega, BMG Labtech). The positive control (100%

hemolysis) was obtained by incubation of hRBCs with demineralized water at the same conditions. Procedures involving human red blood cells have been approved by the Instituto de Higiene e Medicina Tropical Ethics Council (CEIHMT-NOVA; <https://www.ihmt.unl.pt/organizacao/conselho-de-etica/>). All subjects provided informed consent.

### **Live Cell Imaging Using Confocal Microscopy**

Different amounts of **PURE<sub>G4</sub>OEI<sub>48</sub>** were added to 1 mL of bacterial or *Candida* suspension (final concentration  $5 \times 10^5$  CFU mL<sup>-1</sup> and  $1 \times 10^8$  CFU mL<sup>-1</sup> (for the *S. aureus* JE2 strain) and another 1 mL was left untreated as a control. The mixture was incubated for 1 h under a constant stirring, centrifuged (12.000 rpm for 1 min), and resuspended in 1 mL PBS. 1–3  $\mu$ M SYTO 9 (Thermo Fisher Scientific) was added for 30 minutes in the dark (incubation at room temperature) proceeded by a washing step with PBS. Then 2–4  $\mu$ M of TO-PRO-3 iodide (Thermo Fisher Scientific) was added per condition before incubating for additional 15 minutes. This procedure was preceded by a final washing step with PBS. Cells were then placed on microscope slides (making use of Thermo Scientific Gene Frames) covered with a thin layer of agarose (1.2% in PBS). SYTO 9 images were recorded using the 488 nm Ar<sup>+</sup> excitation laser excitation line and the emission was collected at 500–590 nm. TO-PRO-3 iodide images were recorded using 633 nm He-Ne excitation laser line and emission was collected at 645–795 nm. To minimize dye photobleaching during image acquisition the power of each laser line was always kept to a minimum.

### **Scanning Electron Microscopy (SEM) Imaging**

200  $\mu$ L of *Candida* or bacterial suspension (final concentration  $2.5 \times 10^5$  CFU mL<sup>-1</sup> and  $5 \times 10^5$  CFU mL<sup>-1</sup>) containing **PURE<sub>G4</sub>OEI<sub>48</sub>** was added to ibidi 8-well uncoated chambers and another 200  $\mu$ L were left untreated (control samples). The chambers were incubated at 37 °C for 2 h to allow bacterial adherence. Samples were washed three times with PBS and fixed with a 2% (v/v) paraformaldehyde and 2.5% (v/v) glutaraldehyde solution for 30 min at 25 °C. Then, samples were dehydrated with 70% (v/v) ethanol for 10 min, 95% (v/v) ethanol for 10 min, and finally absolute ethanol for 20 min.<sup>24</sup> After complete air-drying, samples were mounted on a carbon conductive adhesive tape followed by gold–palladium coating (Polaron E-5100). SEM images were taken using a

field-emission-gun scanning electron microscopy (FEG-SEM) JEOL 7001F microscope operating at 15 kV with a sample-to-objective working distance of 10 mm.

### Molecular Dynamics Simulation

Coarse-grained (CG) molecular dynamics simulations of interactions between **PURE<sub>G4</sub>OEI<sub>48</sub>** and lipid bilayers (POPC or POPC/POPG) were carried out using GROMACS v2018.3 simulation package<sup>25</sup> with CG Martini 3 force field<sup>26</sup> as it can simulate both polymers and lipid membranes. For **PURE<sub>G4</sub>OEI<sub>48</sub>**, the development of CG bonded and non-bonded parameters were based on all-atom (AA) simulations of the **PURE<sub>G4</sub>** core and the L-OEI-h chain. AA simulations of **PURE<sub>G4</sub>** were carried out in NAMD v2.9<sup>27</sup> parameterized with CGenFF<sup>28</sup> using a previously described protocol.<sup>29</sup> The AA-to-CG mapping made sure to consider the symmetry of the **PURE<sub>G4</sub>OEI<sub>48</sub>**, employing two bead types: a five-to-one mapping for the urea groups and a “five-and-half” bead centered on the tertiary amines (sharing one aliphatic carbon with each of the three neighboring urea beads). Bonded potentials were assigned in a trial-and-error fashion until a good reproduction of AA intramolecular distance and angle distributions was obtained. AA models for the L-OEI-h chains were developed based on the AMBER 99SB forcefield.<sup>30</sup> L-OEI-h was modelled deprotonated, partially protonated (with every other amine deprotonated), and fully protonated. Because AMBER 99SB does not include parameters for secondary amines, charge distributions and torsions were derived from *ab initio* methods for the three protonation states. Partial charges were fit using the Restrained Electrostatic Potential (RESP) method, from structures optimized at the Hartree-Fock level of theory with a 6-31G(d) basis set, and then evaluated at the MP4 level of theory, using the *Gaussian09* software. Torsions were fit by comparing quantum-mechanical and molecular-mechanical potential energies at scanned rotations. L-OEI-h C–N–C oligomer units were mapped to individual CG beads. Termini CG beads correspond only to the C–N atoms and were assigned specific types. Bonded parameters were assigned as for **PURE<sub>G4</sub>**. L-OEI-h chains were then coupled to the 48 terminal amine groups of the **PURE<sub>G4</sub>** dendrimer core, for particles at the three different protonation states. Bilayers of either 100% POPC or 1:3 POPC:POPG were built using the *insane* tool<sup>31</sup> and equilibrated. A hexagonal box of side 70 nm and a *z*-spacing of 20 nm was used. Independently equilibrated particles (one per simulated system) were positioned above the respective bilayer, with a minimum 2 nm clearance, using the structure manipulation features of Visual Molecular Dynamics (VMD).<sup>32</sup> Water beads overlapping

with the particle were removed, and enough Cl<sup>-</sup> and Na<sup>+</sup> ions were added to both neutralize the overall charge and maintain a salt concentration of 150 mM. Minimization and equilibration were performed with a restraint at the central bead of the dendrimer to avoid displacement towards the membrane during these steps. Production simulations were run unrestrained. For all simulations, periodic boundary conditions were used with a 11 Å cut-off for the short-range interactions. Long range electrostatics were treated with the reaction-field method with a relative dielectric constant of 15. Temperature was kept fixed at 300 K using stochastic velocity rescaling with a coupling constant of 1 ps. Pressure was isotropically coupled to 1 bar using the Parrinello-Rahman barostat with a time coupling constant of 12 ps. All production simulations were run for at least 3 μs. For 100% POPC systems, for which little or no interaction was observed, a short preparation step was performed with an acceleration of -1.0 nm ps<sup>-2</sup> on the particle to produce an initial position in close contact with the membrane. This aimed at ensuring that lack of interaction was not due to stochastic factors or kinetic barriers to particle approach. Obtained trajectory results were visually rendered using VMD and analysed using in-house scripts using the MDAnalysis Python package.<sup>33</sup>

### **PURE<sub>G4</sub>OEI<sub>48</sub> Pharmadendrimer Therapeutics of *Galleria mellonella* Larvae**

The assays were based on our methodology.<sup>21</sup> Briefly, *P. aeruginosa* PAO1 and *S. aureus* JE2 overnight liquid cultures were harvested by centrifugation and diluted in PBS (pH 7.4) to obtain 10 CFU and 5x10<sup>5</sup> CFU (respectively for *P. aeruginosa* PAO1 and *S. aureus* JE2) per volume of injection. A micrometer was adapted to control the volume of a microsyringe and inject 5 μL of bacterial suspension into each larva via the hindmost left proleg, previously sanitized with 70% (v/v) ethanol. Following injection, larvae were placed in Petri dishes and stored in the dark at 37 °C. Control larvae were injected with PBS (pH 7.4). A dose of 5 μL of PURE<sub>G4</sub>OEI<sub>48</sub> (up to 4~~8~~ MIC) was administrated at 1 h (in the case of *S. aureus* J2 infection) and 7 h (in the case of *P. aeruginosa* PAO1) post infection. For each condition we used 10 larvae to follow the larval survival over a period of 3 days. Larvae were considered dead when no movement was displayed in response to touch.

### **Statistical Analysis**

All experiments were performed a minimum of three independent assays. Statistical analysis was performed using *Prism GraphPad* software 6.05 (*GraphPad* Software, San



Diego, CA) and the statistical analysis based on the Mantel–Cox test. A  $P$  value  $< 0.05$  was considered statistically significant.

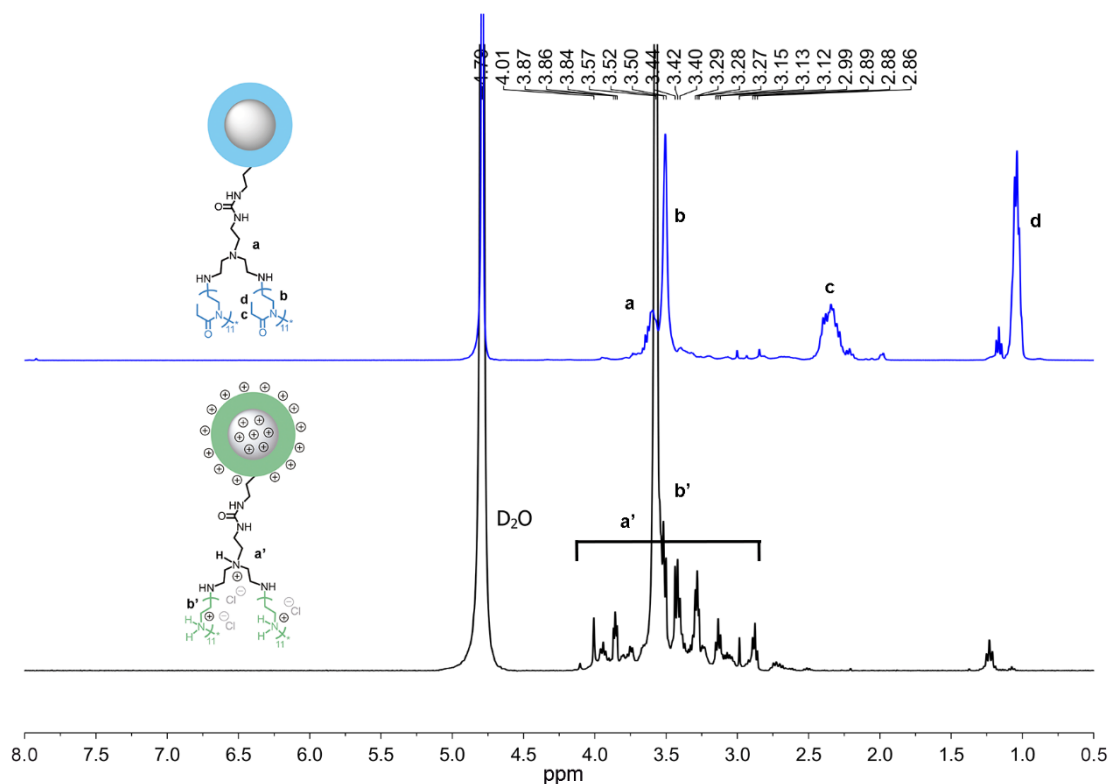


**Fig. S1.**  $^1\text{H}$  NMR spectrum of  $\text{PURE}_{\text{G}_4}\text{OEtOx}_{48}$  (top) and  $\text{PURE}_{\text{G}_4}\text{OEI}_{48}$  phradendrimer (bottom) in  $\text{D}_2\text{O}$ .

**Table S1.** Comparison of the antimicrobial activity of the  $\text{PURE}_{\text{G}_4}\text{OEI}_{48}$  phradendrimer with the structural unit of the core ( $\text{PURE}_{\text{G}_4}$ ) and with the cationic layer (L-OEI-h). The values represent three independent experiments performed with three technical replicates each.

Organism	MIC ( $\mu\text{M}$ )	MIC ( $\mu\text{M}$ )	MIC ( $\mu\text{M}$ )
	$\text{PURE}_{\text{G}_4}\text{OEI}_{48}$	$\text{PURE}_{\text{G}_4}$	L-OEI-h
<i>Staphylococcus aureus</i> JE2 (MRSA)	0.48	>100	>1000
<i>Pseudomonas aeruginosa</i> PAO1	0.96	>100	125
<i>Acinetobacter baumannii</i> C475758	0.96	>100	125
<i>Candida albicans</i> SC5314	0.48	>100	125

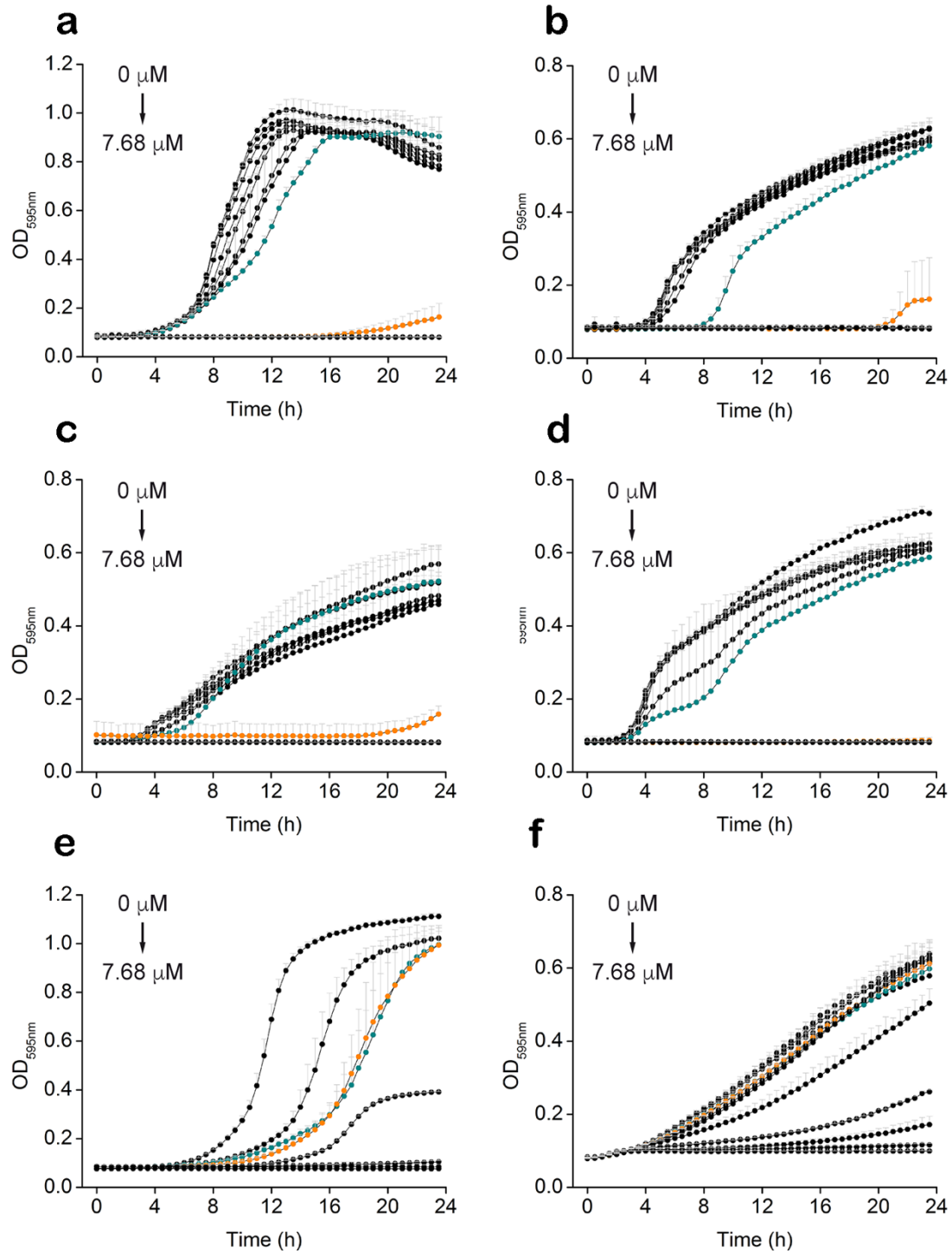


**Fig. S2.** Time-kill curves for Gram-negative bacteria: *P. aeruginosa* PAO1 (a) and *S. enterica* serovar Typhimurium SL1344 (b), Gram-positive bacteria: *S. aureus* ATCC6538 (c) and *S. aureus* JE2 (d) and fungi: *C. galbrata* KUE100 (e) and *C. albicans* SC5314 (f). The curves show the OD reduction before (first curve) after addition of different concentration of **PURE<sub>G4</sub>OEI<sub>48</sub>** pharma-dendrimer (7.68 μM, last curve). Curves near the MIC concentration are represented with a different color (sub-MIC, green color; upper MIC, orange color). OD, optical density. The values represent means of three independent experiments.

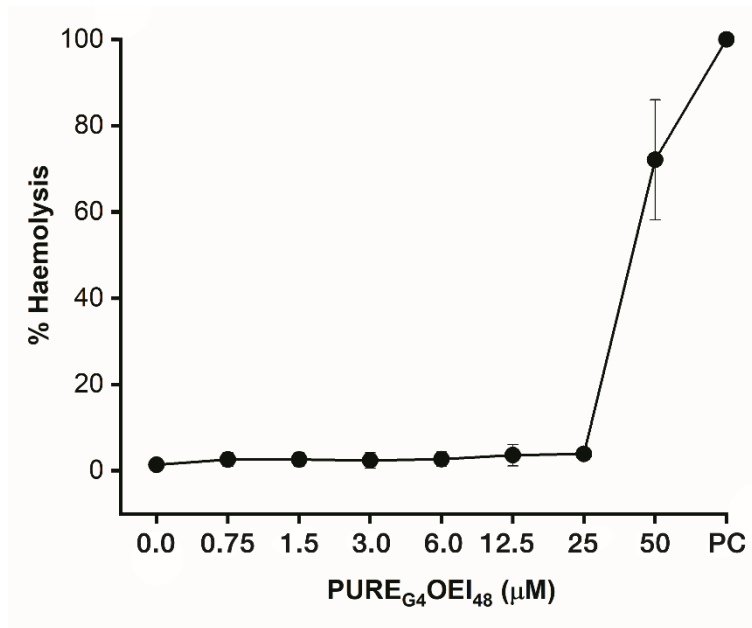


**Fig. S3.** Hemolytic activity of **PURE<sub>G4</sub>OEI<sub>48</sub>** pharomadendrimer after 4 h of incubation. PC, positive control. The values represent means of three independent experiments.

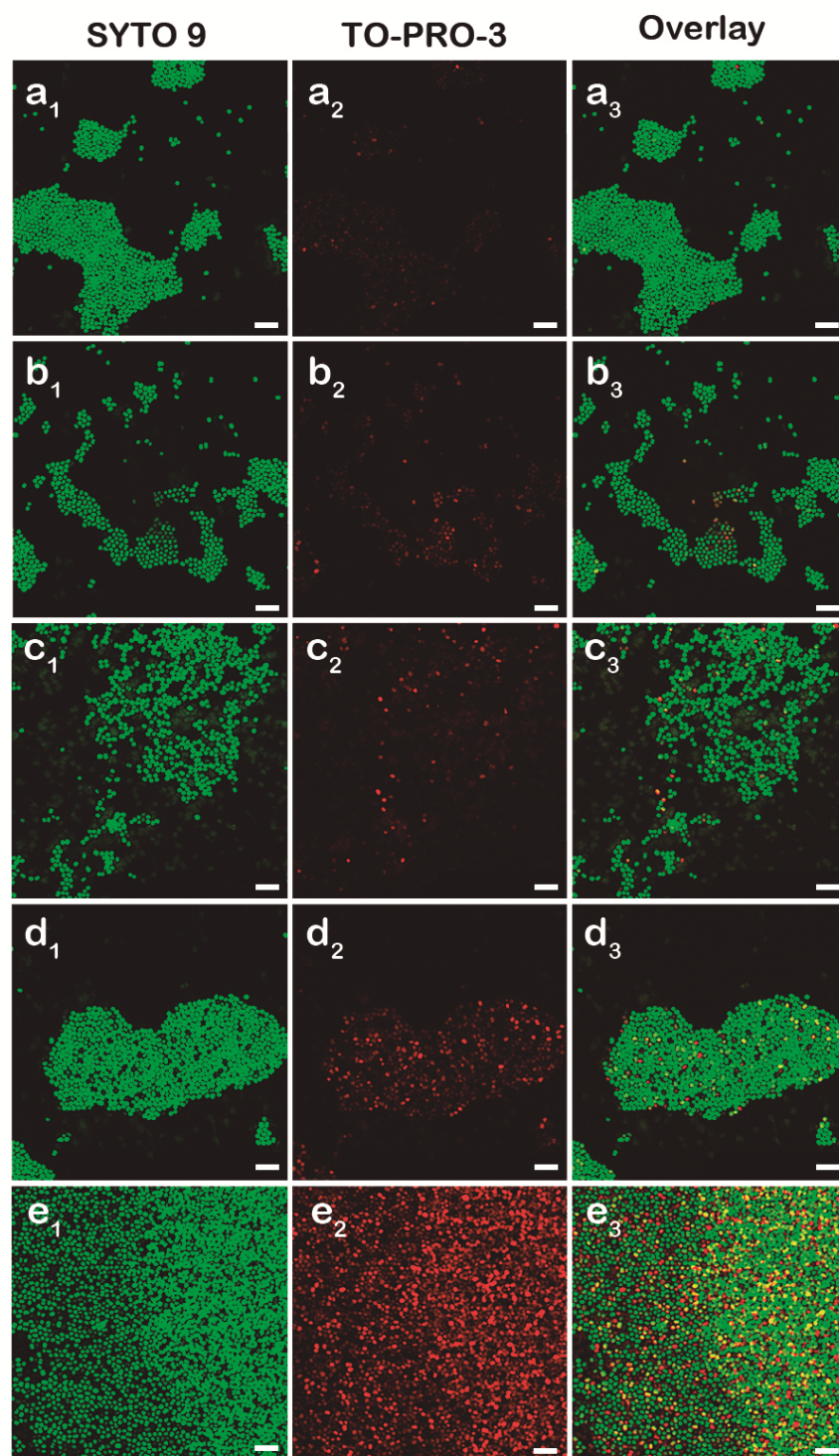


**Fig. S4.** Confocal laser scanning microscopy images of *S. aureus* JE2 Gram-positive cells stained with SYTO 9 (green, left column) and TO-PRO-3 iodide (red, middle column) dyes allowing the discrimination between living and metabolic inactive bacteria cells, respectively. The rows show bacteria incubated at different **PURE<sub>G4</sub>OEI<sub>48</sub>** phradendramer MIC concentrations after 1 h: control, no addition of **PURE<sub>G4</sub>OEI<sub>48</sub>** (a), 1 $\beta$ MIC (b), 2 $\beta$ MIC (c), 3 $\beta$ MIC (d) and 4 $\beta$ MIC (e). All images are representative of three independent experiments (Scale bar: 5  $\mu$ m).

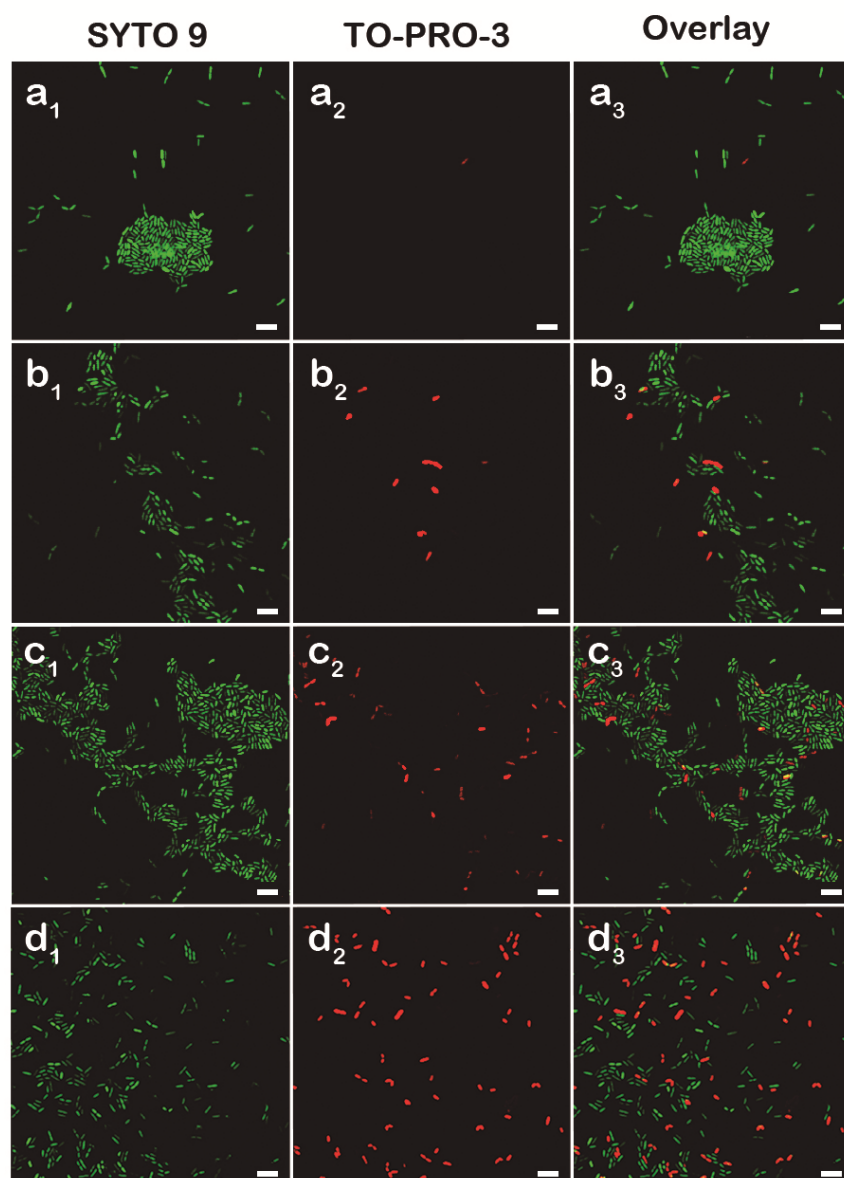


**Fig. S5.** Confocal laser scanning microscopy images of *P. aeruginosa* PAO1 Gram-negative cells treated with serial dilutions of **PURE<sub>G4</sub>OEI<sub>48</sub>** phradendrimer. Bacteria were stained with SYTO 9 (green, left column) and TO-PRO-3 iodide (red, middle column) dyes allowing the discrimination between living and metabolic inactive bacteria cells, respectively. The rows show bacteria incubated at different **PURE<sub>G4</sub>OEI<sub>48</sub>** MIC concentrations after 1 h: control, no addition of **PURE<sub>G4</sub>OEI<sub>48</sub>** (a), 1 $\beta$ MIC (b), 2 $\beta$ MIC (c) and 3 $\beta$ MIC (d). All images are representative of three independent experiments (Scale bar: 5  $\mu$ m).

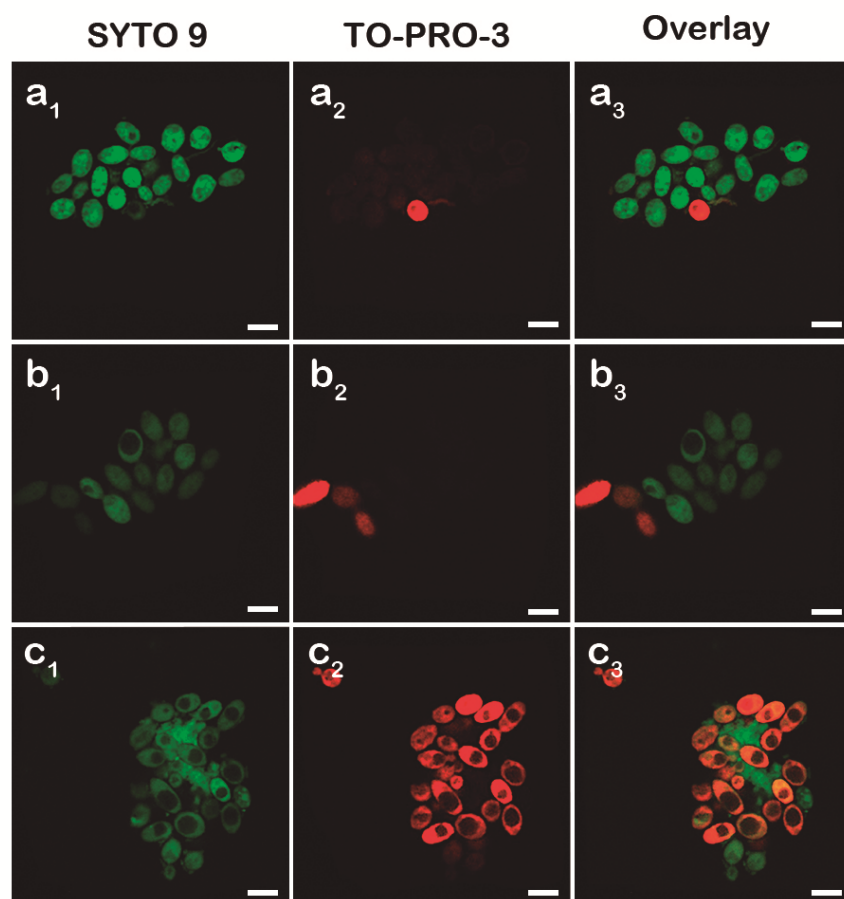


**Fig. S6.** Confocal laser scanning microscopy images of *C. albicans* SC5314 cells stained with SYTO 9 (green, left column) and TO-PRO-3 iodide (red, middle column). The rows show fungi incubated at different **PURE<sub>G4</sub>OEI<sub>48</sub>** MIC concentrations after 1 h: control, no addition of **PURE<sub>G4</sub>OEI<sub>48</sub>** (**a**), 1 $\times$ MIC (**b**) and 2 $\times$ MIC (**c**). All images are representative of three independent experiments (Scale bar: 5  $\mu$ m).



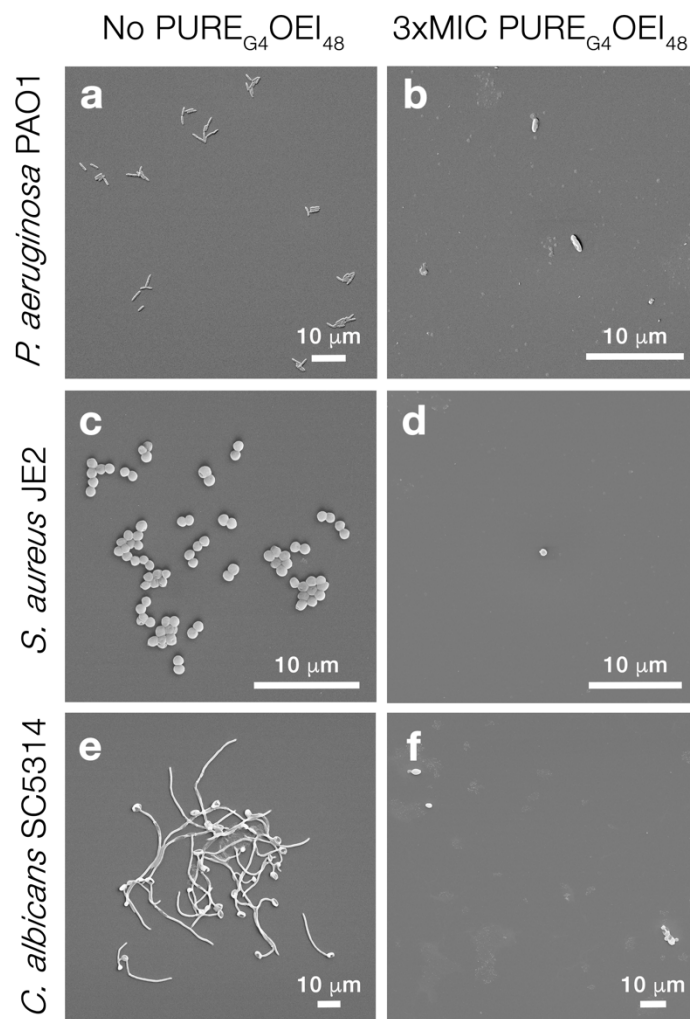


**Fig. S7.** Distribution of microbial cells incubated without or with  $\text{PURE}_{\text{G4}}\text{OEI}_{48}$  pharamadendrimer. Representative scanning electron microscopy (SEM) images of *P. aeruginosa* PAO1, *S. aureus* JE2 and *C. albicans* SC5314 cells grown in the absence or in the presence of 3xMIC  $\text{PURE}_{\text{G4}}\text{OEI}_{48}$ .

**Supplementary Video 1.** Coarse-grained molecular dynamics simulation between a  $\text{PURE}_{\text{G4}}\text{OEI}_{48}$  pharamadendrimer and a POPC-POPG lipid bilayer.

**Supplementary Video 2.** Coarse-grained molecular dynamics simulation between a  $\text{PURE}_{\text{G4}}\text{OEI}_{48}$  pharamadendrimer interaction and a POPC lipid bilayer.

## References

- 1 Restani, R.B., Morgado, P.I., Ribeiro, M.P., Correia, I.J., Aguiar-Ricardo, A., and Bonifácio, V.D.B. Biocompatible polyurea dendrimers with pH-dependent fluorescence. *Angew. Chem. Int. Ed.* 2012, **51**, 5162–5165.
- 2 Pires, R.F., Moro, A., Lourenço, A., Lima, J.C., Casimiro, T. and Bonifácio, V.D.B. Molecular weight determination by luminescent chemoenzymatics. *ChemistrySelect* 2016, **1**, 6818–6822.
- 3 Correia, V.G., Bonifácio, V.D.B., Raje, V.P., Casimiro, T., Moutinho, G., Lobato da Silva, C., Pinho, M.G., and Aguiar-Ricardo, A. Oxazoline-based antimicrobial oligomers: Synthesis by CROP using supercritical CO<sub>2</sub>. *Macromol. Biosci.* 2011, **11**, 1128–1137.
- 4 Restani, R.B., Conde, J., Pires, R.F., Martins, P., Fernandes, A.R., Baptista, P.V., Bonifácio, V.D.B. and Aguiar-Ricardo, A. POxylated polyurea dendrimers: Smart core-shell vectors with IC<sub>50</sub> lowering capacity. *Macromol. Biosci.* 2015, **15**, 1045–1051.
- 5 Diekema, D.J., Richter, S.S., Heilmann, K.P., Dohrn, C.L., Riahi, F., Tendolkar, S., McDanel, J.S. and Doern, G.V. Continued emergence of USA300 methicillin-resistant *Staphylococcus aureus* in the United States: Results from a nationwide surveillance study. *Infect. Control Hosp. Epidemiol.* 2014, **35**, 285–292.
- 6 Tettelin H., Nelson K.E., Paulsen I.T., Eisen J.A., Read T.D., Peterson S., Heidelberg J., DeBoy R.T., Haft D.H. and Dodson R.J. et al. Complete genome sequence of a virulent isolate of *Streptococcus pneumoniae*. *Science* 2001, **293**, 498–506.
- 7 Stover, C.K., Pham, X.Q., Erwin, A.L., Mizoguchi, S.D., Warrenner, P., Hickey, M.J., Brinkman, F.S.L., Hufnagle, W.O., Kowalik, D.J., Lagrou, M. et al. Complete genome sequence of *Pseudomonas aeruginosa* PAO1, an opportunistic pathogen. *Nature* 2000, **406**, 959–964.
- 8 Manageiro, V., Jones-Dias, D., Ferreira, E., Louro, D., Antimicrobial Resistance Surveillance Program in Portugal, Caniça, M. Genetic diversity and clonal evolution of carbapenem-resistant *Acinetobacter baumannii* isolates from Portugal and the dissemination of ST118. *Int. J. Antimicrob. Agents.* 2012, **40**, 398–403.
- 9 Holden M.T., Seth-Smith H.M., Crossman L.C., Sebahia M., Bentley S.D., Cerdeño-Tárraga A.M., Thomson N.R., Bason N., Quail M.A. and Sharp S. et al.



- The genome of *Burkholderia cenocepacia* J2315, an epidemic pathogen of cystic fibrosis patients. *J. Bacteriol.* 2009, **191**, 261–277.
- 10 Gillum, A. M., Tsay, E. Y. H. and Kirsch, D. R. Isolation of the *Candida albicans* gene for orotidine-5'-phosphate decarboxylase by complementation of *S. cerevisiae* *ura3* and *E. coli* *pyrF* mutations. *Mol. Genet.* 1984, **198**, 179–182.
  - 11 Ueno, K., Uno, J., Nakayama, H., Sasamoto, K., Mikami, Y. and Chibana, H. Development of a highly efficient gene targeting system induced by transient repression of YKU80 expression in *Candida glabrata*. *Eukaryot. Cell.* 2007, **6**, 1239–1247.
  - 12 Pais, P., Vagueiro, S., Mil-Homens, D., Pimenta, A. I., Viana, R., Okamoto, M., Chibana, H., Fialho, A.M. and Teixeira, M.C. A new regulator in the crossroads of oxidative stress resistance and virulence in *Candida glabrata*: The transcription factor CgTog1. *Virulence* 2020, **11**, 1522–1538.
  - 13 Pankey, G.A. and Sabath, L.D. Clinical relevance of bacteriostatic versus bactericidal mechanisms of action in the treatment of Gram-positive bacterial infections. *Clin. Infect. Dis.* 2004, **38**, 864–870.
  - 14 Tang, W.H., Wang, C.F. and Liao, Y.D. Fetal bovine serum albumin inhibits antimicrobial peptide activity and binds drug only in complex with  $\alpha$ 1-antitrypsin. *Sci. Rep.* 2021, **11**, 1267.
  - 15 Dias, S.A., Freire, J. M., Pérez-Peinado, C., Domingues, M.M., Gaspar, D., Vale, N., Gomes, P., Andreu, D., Henriques, S.T., Castanho, M., and Veiga, A.S. New potent membrane-targeting antibacterial peptides from viral capsid proteins. *Front. Microbiol.* 2017, **8**, 775.
  - 16 Mangoni, M.L., Papo, N., Barra, D., Simmaco, M., Bozzi, A., Di Giulio, A., Rinaldi, A.C. Effects of the antimicrobial peptide temporin L on cell morphology, membrane permeability and viability of *Escherichia coli*. *Biochem. J.* 2004, **380**, 859–865.
  - 17 Mil-Homens, D., Pinto, S.N., Matos, R. G., Arraiano, C. and Fialho, A.M. *Burkholderia cenocepacia* K56-2 trimeric autotransporter adhesin BcaA binds TNFR1 and contributes to induce airway inflammation. *Cell Microbiol.* 2017, **19**.
  - 18 Cozens A.L., Yezzi M.J., Kunzelmann K., Ohrui T., Chin L., Eng K., Finkbeiner W.E., Widdicombe J.H. and Gruenert D.C. CFTR expression and chloride

- secretion in polarized immortal human bronchial epithelial cells. *Am. J. Respir. Cell Mol. Biol.* 1994, **10**, 38–47.
- 19 Xu, M., McCanna, D.J. and Sivak, J.G. Use of the viability reagent PrestoBlue in comparison with alamarBlue and MTT to assess the viability of human corneal epithelial cells. *J. Pharmacol. Toxicol. Methods* 2015, **71**, 1–7.
- 20 Mil-Homens, D., Martins, M., Barbosa, J., Serafim, G., Sarmiento, M.J., Pires, R.F., Rodrigues, V., Bonifácio, V.D.B., and Pinto, S.N. Carbapenem-resistant *Klebsiella pneumoniae* clinical isolates: *In vivo* virulence assessment in *Galleria mellonella* and potential therapeutics by polycationic oligoethyleneimine. *Antibiotics* 2021, **10**, 56.
- 21 Mil-Homens, D., Bernardes, N. and Fialho, A.M. The antibacterial properties of docosahexaenoic omega-3 fatty acid against the cystic fibrosis multiresistant pathogen *Burkholderia cenocepacia*. *FEMS Microbiol. Lett.* 2012, **328**, 61–69.
- 22 Zielińska, P., Staniszevska, M., Bondaryk, M., Koronkiewicz, M. and Urbańczyk-Lipkowska, Z. Design and studies of multiple mechanism of anti-*Candida* activity of a new potent Trp-rich peptide dendrimers, *Eur. J. Med. Chem.* 2015, **105**, 106-119.
- 23 Nogueira, F., Diez, A., Radfar, A., Pérez-Benavente, S., do Rosario, V.E., Puyet, A. and Bautista, J.M. Early transcriptional response to chloroquine of the *Plasmodium falciparum* antioxidant defence in sensitive and resistant clones. *Acta Tropica* 2010, **114**, 109–115.
- 24 Alves, M.M., Cunha, D.V., Santos, C.V., Mira, N.P., Montemor, M.F. *In vitro* corrosion behaviour and anti-*Candida* spp. activity of Zn coated with ZnO-nanostructured ‘Anastacia’ flowers. *J. Mater. Chem. B* 2016, **4**, 4754–4761.
- 25 Abraham, M., Hess, B., van der Spoel, D. and Lindahl, E. GROMACS User Manual, 2018.
- 26 Marrink S.J., Risselada H.J., Yefimov S., Tieleman D.P. and de Vries A.H. The MARTINI force field: Coarse grained model for biomolecular simulations. *J. Phys. Chem. B* 2007, **111**, 7812–7824.
- 27 Phillips J.C., Braun R., Wang W., Gumbart J., Tajkhorshid E., Villa E., Chipot C., Skeel R.D., Kalé L., Schulten K. Scalable molecular dynamics with NAMD. *J. Comput. Chem.* 2005, **26**, 1781–1802.
- 28 Vanommeslaeghe K., Hatcher E., Acharya C., Kundu S., Zhong S., Shim J., Darian E., Guvench O., Lopes P., Vorobyov I., Mackerell A.D. Jr. CHARMM

- general force field: A force field for drug-like molecules compatible with the CHARMM all-atom additive biological force fields. *J. Comput. Chem.* 2009, **31**, 671–690.
- 29 Martinho, N., Silva, L.C., Florindo, H.F., Brocchini, S., Zloh, M. and Barata, T.S. Rational design of novel, fluorescent, tagged glutamic acid dendrimers with different terminal groups and in silico analysis of their properties. *Int. J. Nanomedicine* 2017, **12**, 7053–7073.
- 30 Hornak V., Abel R., Okur A., Strockbine B., Roitberg A., Simmerling C. Comparison of multiple Amber force fields and development of improved protein backbone parameters. *Proteins* 2006, **65**, 712–725.
- 31 Wassenaar, T.A., Ingólfsson, H.I., Böckmann, R.A., Tieleman, D.P. and Marrink, S.J. Computational lipidomics with insane: A versatile tool for generating custom membranes for molecular simulations. *J. Chem. Theory Comput.* 2015, **12**, 2144–2155.
- 32 Humphrey, W., Dalke, A. and Schulten, K. VMD: Visual molecular dynamics. *J. Mol. Graph.* 1996, **14**, 33–38.
- 33 Michaud-Agrawal N., Denning E.J., Woolf T.B., Beckstein O. MDAAnalysis: A toolkit for the analysis of molecular dynamics simulations. *J. Comput. Chem.* 2011, **32**, 2319–2327.